Dynamic-Range Compression in Surface-Coil MRI

Robert B. Lufkin[1]
Tom Sharpless[2]
Bonnie Flannigan[1]
William Hanafee[1]

The large dynamic range in signal intensity present in MR surface-coil images makes proper windowing and photography difficult. By removing the low-spatial frequency information caused by variations in surface-coil field intensity from the high-spatial frequency information containing the image data, a considerable compression of this dynamic range of signal intensity is possible. To accomplish this, a technique was implemented on a digital computer for use with MR surface-coil image data. The compression was done as a postprocessing option after the patient scan had been completed and therefore did not alter actual scan times. Although the image signal-to-noise was not altered, the ease of photography for most images was improved. Thus, digital dynamic-range compression is a practical technique to aid in surface-coil MRI studies.

Initially used for in vivo phosphorus spectroscopy, planar surface coils have recently been applied to proton imaging, which results in a dramatic improvement in image quality for small, superficial structures over conventional coil types [1–8]. Surface coils have low noise and high sensitivity to nearby signals, which drop off rapidly beyond one radius from the coil center [9–10]. The rapid dropoff in signal with planar and other noncircumferential surface coils results in image-intensity variation, which makes proper windowing and photography difficult. To view regions from various parts of the field, two or more separately windowed images may be necessary to optimally display the proper signal intensities.

The application of a nonlinear dynamic-range compression technique to improve the appearance and ease of surface-coil image display is described below.

Methods

A computer program was written to compress the dynamic range of surface-coil MR images after scanning was completed as a postprocessing function. Each image was rescaled logarithmically and then passed through a linear filter to reduce the multiplicative low-spatial frequency terms introduced by the sensitivity function of the surface coils.

The high-pass filter function was accomplished by calculating the difference between the original image signal (S_0) and the low-pass filtered signal. This preserves the high spatial-frequency information that is important to the radiologist. After filtering, the signal is then exponentiated and the image reformed with compression of the intensity dynamic range. The final output image signal (S) is represented by the following relation:

$$S = \exp(\log(S_0) - \text{lowpass filter}(\log(S_0))) \quad (1)$$

Images were obtained on a 0.3-T permanent magnet imaging system (FONAR β-3000, Melville, NY). A 2D-FT multislice spin-echo technique with a repetition time (TR) of 500 msec and an echo delay time (TE) of 28 msec was used. The images were acquired on either a 256 × 256 or 512 × 512 matrix and displayed on a 512 × 512 image matrix. High-resolution image acquisition was possible with pixels as small as 0.375 mm^2. Slice thickness was variable down to 3 mm with an interslice gap of 2 mm. Four signal averages were generally

Received December 11, 1985; accepted after revision April 10, 1986.

This work was supported by U.S. Public Health Service Grant 1K08 CA 00979-01 from the National Cancer Institute, Department of Health and Human Services, and by the University of California Cancer Research Coordinating Committee funds.

[1] Department of Radiological Sciences, UCLA School of Medicine, Los Angeles, CA 90024. Address reprint requests to R. B. Lufkin.

[2] FONAR Corporation, Melville, NY 11747.

AJR 147:379–382, August 1986
0361–803X/86/1472–0379

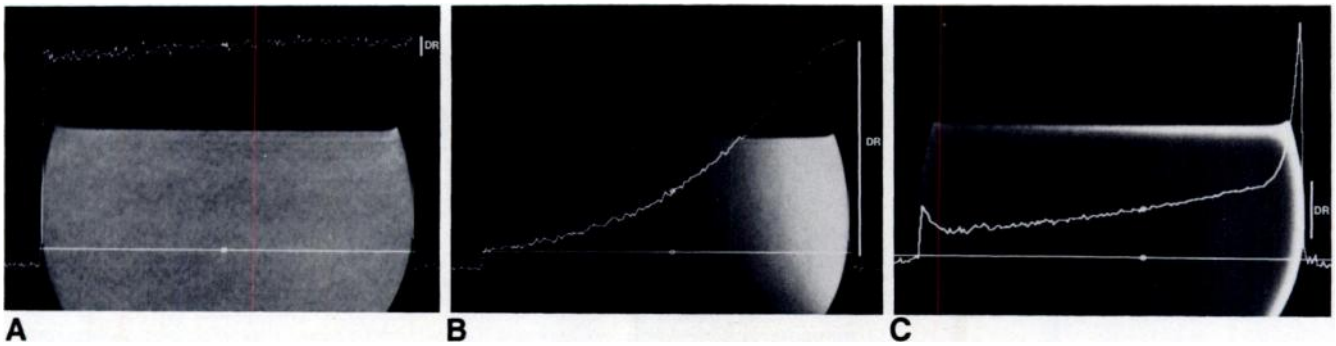

Fig. 1.—Comparison of signal detection of standard circumferential and planar coils applied to uniform 2.5-mM NiCl solution phantom. Curves are plots of signal intensity through midportion of phantom. All images are SE/500/28, axial, 4 mm thick, with 0.75 × 0.75-mm pixels obtained with four signal averages. Dynamic range of image intensity is shown (DR). **A**, Circumferential head coil (27 cm) shows moderate amount of noise (as indicated by mottled image appearance and irregular baseline plot), but shows fairly good deep-signal detection. A relatively narrow dynamic range is present. **B**, 14-cm planar surface coil shows low noise and high superficial signal detection but rapid signal dropoff with increasing distance from coil surface. This results in a large-image dynamic range that makes appropriate windowing and photography difficult. **C**, Planar coil image **B** after signal intensity dynamic-range compression. Dynamic range is considerably smaller. Although signal of deep structures was increased, so was noise for these regions. Therefore, no net change in signal-to-noise is apparent. Presence of excess edge brightness is due to lack of information about sensitivity function where signal is absent.

used resulting in an imaging time of 8.5 min for seven slices with the standard 256 × 256 acquisition matrix.

A uniform phantom filled with 2.5 mM NiCl (T1 = 460 msec at 0.3 T) produces a consistently high signal using this pulse sequence (SE/500/28). Normal volunteers and patients with disease were also scanned after giving informed consent. Various planar surface coils as well as conventional circumferential head and body coils were used with the phantom and normal volunteers. When used, surface coils functioned as receiver coils only. RF transmission was accomplished through the standard body coil.

The resulting images from both coil types were studied. Intensity plots across the image were made to display the dynamic range of signal intensity before and after dynamic-range compression.

Results

Typical signal-intensity dynamic ranges for the surface-coil phantom images were 11:1 and 1:1 in an image obtained with a circumferential coil (Fig. 1). After dynamic-range compression, the surface-coil phantom image range was reduced to 2.3:1. While the signal from deep structures increased, the noise was also increased proportionately. Effectively no net change in the signal-to-noise ratio occurred. Analysis excludes the regions near the phantom edges, where the filter exhibits an unavoidable overshoot (Fig. 1). Over most of the phantom area, a dynamic-range compression by a factor of almost five was achieved.

The wide dynamic range in clinical surface-coil images necessitated careful windowing or photography at several windows and levels in order to optimally display all the information in the image (Figs. 2A and 3A). After dynamic range compression, viewing or photography at multiple window settings was not necessary (Figs. 2B and 3B).

Discussion

Surface coils are a marked improvement over standard body and head coils for certain applications. Signal-to-noise in MR receiver coils is represented by the following relation:

$$S/N \approx \sqrt{\eta \times ((\text{frequency})/(a + b\sqrt{\text{frequency}} + d \times \text{frequency}^2))}, \quad (2)$$

where η is the filling factor of the coil and depends on the relationship of the patient to the coil. The second term represents the coil-quality factor. a is proportional to the DC resistivity of the coil material (copper), b is proportional to the RF resistivity of the coil material, and d is dependent on coil loading by the patient.

At the higher frequencies of 12.8 Mhz (0.3 T) and greater, which are currently used for imaging, the frequency-squared term (i.e., the effects of coil loading by the patient) dominates in the denominator of the quality-factor term (equation 2) and consequently determines the signal-to-noise in these coils. This is true for all coils whose design has been optimized such that the noise due to coil materials is minimized ($Q_{empty} \gg Q_{loaded}$).

Significant improvement in coil-loading-and-filling factor with surface coils over standard body coils results in markedly improved signal-to-noise and image quality and allows for production of thin sections and high-resolution images, which are essential for many applications.

Planar and other noncircumferential surface coils have a marked loss of signal beyond one radius from the coil center [11, 12]. Dropoff in signal intensity limits the effectiveness of this coil when imaging deeper structures and results in a large dynamic range of intensity that is difficult to view with a single setting of window width and level.

The compression technique is an example of homomorphic filtering, a broad class of signal-processing techniques for the reduction of dynamic range. Related methods have been used for some time in speech and seismic-wave analysis to separate multiplicative components of signals, as well as for image enhancement [13, 14].

Homomorphic filtering and unsharp masking are very similar; however, homomorphic filtering operates on the log of the

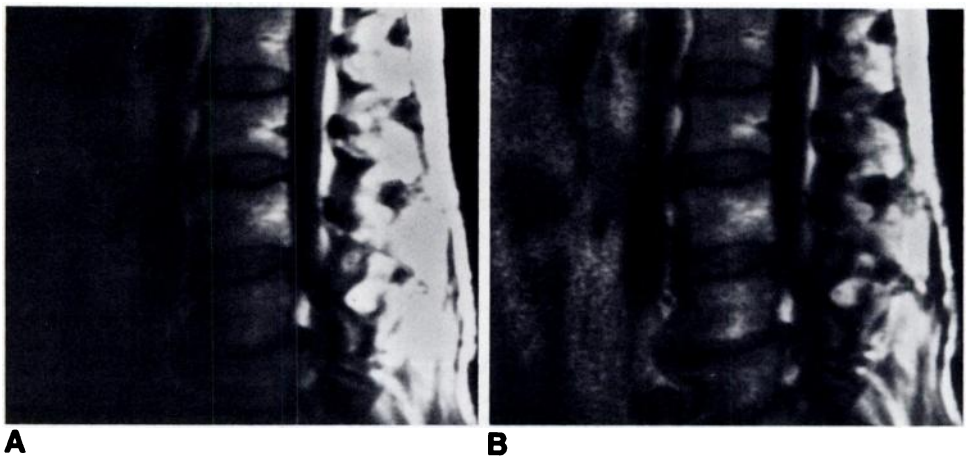

Fig. 2.—Sagittal scan through normal lumbar spine using a planar spine surface coil. Imaging parameters were SE/500/28, 4 mm thick, with 0.75 × 0.75-mm pixels obtained with four signal averages. **A**, Windowed to demonstrate spinal canal (window level = 750, window width = 1800). This region is optimally seen at expense of deeper and more superficial tissues. **B**, Same scan as **A** after image intensity dynamic-range compression (window level = 750, window width = 1800). Now all depths of tissue are fairly well seen and may be evaluated on one image.

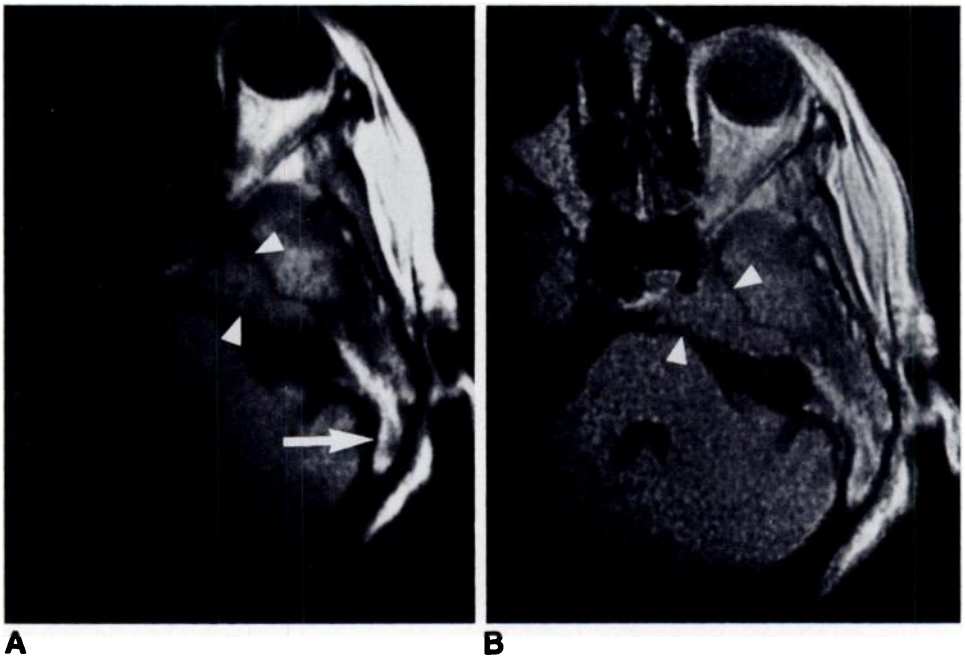

Fig. 3.—Axial image through temporal bone obtained using a planar surface coil (SE/500/28). **A**, Image with standard display format shows high signal in region of mastoid air cells indicating otomastoiditis (*arrow*). A deeper abnormality is less obvious (*arrowheads*). **B**, Same image after dynamic-range compression brings up signal intensity of abnormality at margin of sensitivity of coil. Mass present in clivus (*arrowheads*) displaces ipsilateral carotid artery anteriorly. Diagnosis was metastatic adenocarcinoma.

image data. Therefore, whereas unsharp masking is a linear process, homomorphic filtering is nonlinear.

Variation in signal with depth on surface-coil images is a low spatial-frequency sensitivity function that multiplies the desired signal. The important anatomic and morphologic clinical information in the signal is largely a high spatial frequency function. Therefore, if the low spatial-frequency intensity variation could be filtered out while preserving the high spatial frequency image information, the great variation in image intensity would be reduced. The logarithm of the image converts the product of two functions into the sum of their logarithms, which can be separated by a linear filter. Then, exponentiating the result yields the compressed image.

The compression technique is a general process that works without having to specify the signal dropoff function of the surface coil. Of course, this function varies depending on the size and shape of the particular surface coil used. The technique is also digital and is therefore easily implemented on most computer systems; in fact, it is one of the few digital-image processing algorithms without a simple photographic analog.

However, the dynamic-range compression method cannot compress all the way to the edge of an image because information regarding the sensitivity function is not available where there is no signal. While evident in the phantom images shown here, excess edge brightness does not seem to be a problem in compressed clinical images.

REFERENCES

1. Ackerman JJH, Grove TH, Wong GG, Gadian DG, Radda GK. Mapping of metabolites in whole animals by ^{31}P NMR using

surface coils. *Nature* **1980**;283:167–170
2. Gadian DG. *Nuclear magnetic resonance and its applications to living systems*. Oxford, Eng: Clarendon Press, **1982**
3. Bernardo ML, Cohen AJ, Lauterbur PC. Radiofrequency coil designs for nuclear magnetic zeugmatographic imaging. In: *IEEE proceedings of the international workshop on physics and engineering in medical imaging*. March **1982**:277–284
4. Axel L. Surface coil magnetic resonance imaging. *J Comput Assist Tomogr* **1984**;8:381–384
5. Reicher M, Bassett L, Rauschning W, Gold R, Lufkin R, Glenn W. MRI of the knee. *AJR*, in press
6. Lufkin R, Hanafee W. Application of surface coils to NMR anatomy of the larynx. *AJNR* **1985**;6:491–497
7. Schenck JF, Foster TH, Henkes JL, et al. High field surface coil MR imaging of localized anatomy. *AJNR* **1985**;6:181–186
8. Schenck JF, Hart HR, Foster TH, et al. Improved MR imaging of the orbit at 1.5 T with surface coils. *AJNR* **1985**;6:193–196
9. Smyth WR. *Static and dynamic electricity*. New York: McGraw-Hill, **1968**
10. Hoult DI, Richards RE. Signal to noise ratio of nuclear magnetic resonance experiment. *J Mag Res* **1976**;24:71–85
11. Fitzsimmons JR, Thomas RG, Mancuso AA. Proton imaging with surface coils on a 0.15-T resistive system. *J Mag Res Med* **1985**;2:180–185
12. Lufkin RB, Votruba J, Reicher M, Bassett L, Smith D, Hanafee W. Solenoid surface coils in MRI. *AJR* **1986**;146:409–412
13. Oppenheim AV, Schafer RW, Stockham TG. Nonlinear filtering of multiplied and convolved signals. *Proc IEEE* **1968**;56:1264–1291
14. Oppenheim AV, Schafer RW. *Digital signal processing*. Englewood Cliffs, NJ: Prentice-Hall, **1975**:480–529